



## On the properties of poly(isoprene-b-ferrocenylmethyl methacrylate) block copolymers

Chernyy, Sergey; Kirkensgaard, Jacob Judas Kain; Bakke, Anders; Mortensen, Kell; Almdal, Kristoffer

*Published in:*  
Polymer

*Link to article, DOI:*  
[10.1016/j.polymer.2017.11.036](https://doi.org/10.1016/j.polymer.2017.11.036)

*Publication date:*  
2017

*Document Version*  
Peer reviewed version

[Link back to DTU Orbit](#)

*Citation (APA):*  
Chernyy, S., Kirkensgaard, J. J. K., Bakke, A., Mortensen, K., & Almdal, K. (2017). On the properties of poly(isoprene-b-ferrocenylmethyl methacrylate) block copolymers. *Polymer*, 133, 129-136.  
<https://doi.org/10.1016/j.polymer.2017.11.036>

---

### General rights

Copyright and moral rights for the publications made accessible in the public portal are retained by the authors and/or other copyright owners and it is a condition of accessing publications that users recognise and abide by the legal requirements associated with these rights.

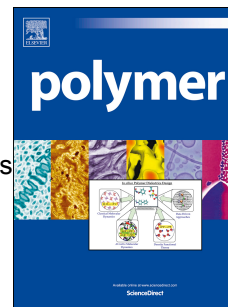
- Users may download and print one copy of any publication from the public portal for the purpose of private study or research.
- You may not further distribute the material or use it for any profit-making activity or commercial gain
- You may freely distribute the URL identifying the publication in the public portal

If you believe that this document breaches copyright please contact us providing details, and we will remove access to the work immediately and investigate your claim.

# Accepted Manuscript

On the properties of poly(isoprene-*b*-ferrocenylmethyl methacrylate) block copolymers

Sergey Chernyy, Jacob Judas Kain Kirkensgaard, Anders Bakke, Kell Mortensen, Kristoffer Almdal



PII: S0032-3861(17)31093-5

DOI: [10.1016/j.polymer.2017.11.036](https://doi.org/10.1016/j.polymer.2017.11.036)

Reference: JPOL 20149

To appear in: *Polymer*

Received Date: 27 September 2017

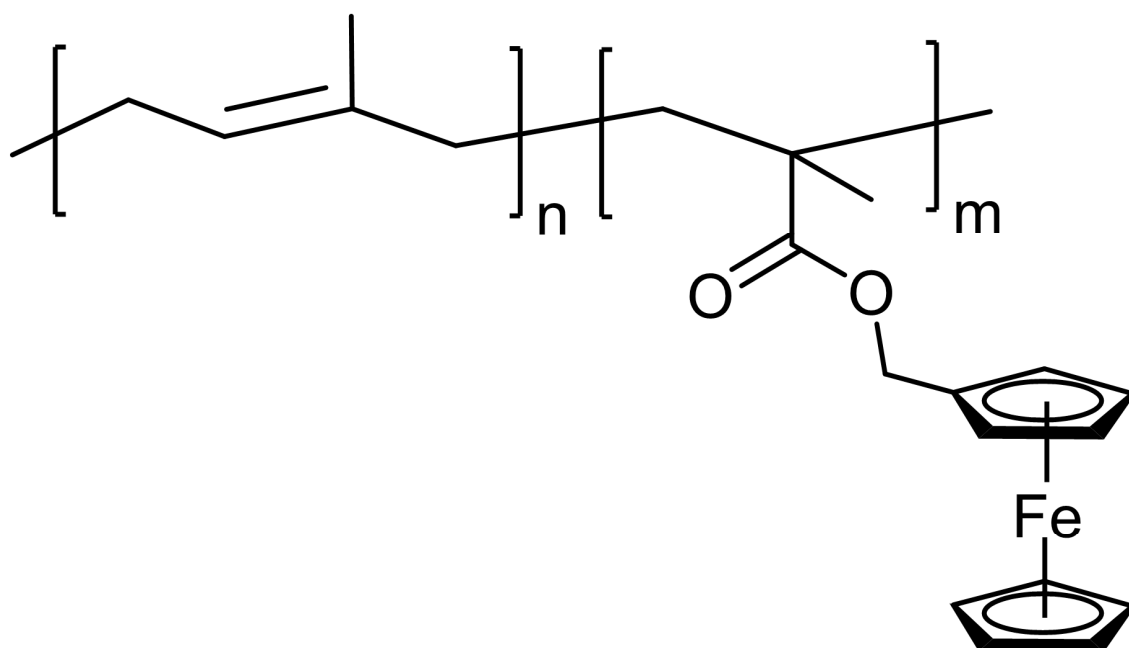
Revised Date: 11 November 2017

Accepted Date: 15 November 2017

Please cite this article as: Chernyy S, Kirkensgaard JJK, Bakke A, Mortensen K, Almdal K, On the properties of poly(isoprene-*b*-ferrocenylmethyl methacrylate) block copolymers, *Polymer* (2017), doi: 10.1016/j.polymer.2017.11.036.

This is a PDF file of an unedited manuscript that has been accepted for publication. As a service to our customers we are providing this early version of the manuscript. The manuscript will undergo copyediting, typesetting, and review of the resulting proof before it is published in its final form. Please note that during the production process errors may be discovered which could affect the content, and all legal disclaimers that apply to the journal pertain.

$$\chi = 0.12 + 0.19/T$$



ACCEPTED

1 **On the properties of poly(isoprene-*b*-ferrocenylmethyl methacrylate) block**  
2 **copolymers**

3  
4 Sergey Chernyy,<sup>1\*</sup> Jacob Judas Kain Kirkensgaard,<sup>2</sup> Anders Bakke,<sup>2</sup> Kell Mortensen,<sup>2</sup> Kristoffer  
5 Almdal<sup>1</sup>

6  
7 <sup>1</sup>*Technical University of Denmark, DTU Nanotech - Department of Micro- and*  
8 *Nanotechnology, Produktionstorvet, 2800 Kgs. Lyngby, Denmark*

9 <sup>2</sup>*Niels Bohr Institute, University of Copenhagen, 2100 Copenhagen, Denmark*

10  
11 **\*Corresponding author**

12 Sergey Chernyy

13 Email: sergeychernyy@gmail.com

14  
15 **Keywords**

16 Ferrocenylmethyl methacrylate (FMMA), poly(1,4-isoprene), anionic polymerization, diblock  
17 copolymers, Flory-Huggins interaction parameter, rheology, order-disorder transition.

**18 Abstract**

19 By combining poly(1,4-isoprene) (PI) with poly(ferrocenylmethyl methacrylate) (PFMMA) in a  
20 diblock copolymer structure by means of anionic polymerization we obtained narrowly dispersed  
21 PI-*b*-PFMMA copolymers with molecular weight ranging from 13000 to 62000 g/mol. The  
22 products were stable up to 228 °C, according to thermal gravimetry, which allowed us to further  
23 investigate their viscoelastic and X-ray scattering properties at elevated temperature by rheology  
24 and SAXS, respectively. For PI-*b*-PFMMA with total molecular weight 13400 g/mol a phase  
25 transition at 105 °C was identified leading to the segmental mixing at  $T > 105$  °C and microphase  
26 separation at  $T < 105$  °C. The microphase separated morphology acquired hexagonally packed  
27 cylinder (HEX) microstructure in bulk. The explanation of the ordered HEX morphology was  
28 derived from a quantification of the thermodynamic immiscibility between PI and PFMMA  
29 segments via random phase approximation theory yielding generally accepted dependency of the  
30 Flory-Huggins interaction parameter ( $\chi$ ) on temperature.

**31 Introduction**

32 Methacrylate derivatives of ferrocene have attracted scientific interest since 1970 due to their  
33 ability to undergo rapid free radical polymerization and their numerous technologically important  
34 properties which originate from the organometallic group [1-3]. Polymers bearing ferrocenyl groups  
35 are redox-active and therefore widely applied in the areas of electrochemical sensing, molecular  
36 recognition and energy storage [4-6]. Linear and nonlinear optical properties could be modulated by  
37 linking ferrocene donors with acceptors [7]. Pyrolysis of the ferrocene-based polymers affords  
38 ceramics which are magnetically susceptible while oxygen plasma oxidation of thin films allows a  
39 direct access to nanostructured substrates [8-10].

40 The most typical example of methacrylate derivatives of ferrocene is poly(ferrocenylmethyl  
41 methacrylate) [PFMMA] which has been homopolymerized and copolymerized with a range of  
42 standard monomers [11]. Soon thereafter (1977) anionic homopolymerization of FMMA was  
43 reported by Pittman and Hirao affording lower polydispersity (PDI) compared to free-radically

44 produced samples [12]. Surprisingly, no reports on successful anionic block copolymerization of  
45 FMMA were published until recently probably due to the challenging monomer purification step  
46 involved. In 2009 Gallei et al. studied PS-*b*-FMMA [poly(styrene)] and found that due to rather  
47 weak intersegment interactions the morphology of the produced diblock copolymers remained  
48 largely disordered in the bulk state [13]. It is worth mentioning in this context that the measure of  
49 segment-segment interaction energy is best described by the Flory-Huggins interaction parameter  
50 ( $\chi$ ). When  $\chi$  is positive for a given diblock copolymer heterocontacts between segments are  
51 energetically unfavorable and demixing occurs. The demixing at a segmental level leads to  
52 microphase separation at the nanoscale, the extent of which depends on the product of  $\chi$  and the  
53 total number of segments in a diblock copolymer ( $\chi N$ ). When  $\chi N \gg 10.5$  strong segregation takes  
54 place and equilibrium morphologies have sharp boundaries between nanodomains while for  $\chi N$   
55 close to but larger than 10.5 partial segmental mixing at the interfaces leads to more diffuse  
56 boundaries [14-16]. We have shown in our previous report<sup>2</sup> that combining in a diblock copolymer  
57 structure a perfluorinated methacrylate as a first block and PFMMA as a second block infers well-  
58 ordered bulk and surface morphologies, even for low molecular weight, which indicates strong  
59 segregation/incompatibility between the two blocks.

60 The aim of these studies is to assess in a quantitative manner the intersegment incompatibility of  
61 PI-*b*-PFMMA [poly(1,4-isoprene)] diblock copolymers. For this purpose a series of PI-*b*-PFMMA  
62 diblock copolymers were synthesized and PI-PFMMA interactions ( $\chi_{\text{PI-PFMMA}}$ ) were ascertained  
63 using random phase approximation (RPA) theory. The choice of PI as a first block was not  
64 accidental. We [2] and others [13] have shown that no well-ordered morphologies are attainable  
65 when using classical styrene and methyl methacrylate (MMA) monomers to produce PMMA-*b*-  
66 PFMMA and PS-*b*-PFMMA copolymers. The third classical monomer is isoprene which is  
67 inexpensive and its polymerization kinetics is well established. Exploiting this advantage along with  
68 the fact that PI-*b*-PFMMA could undergo microphase separation affording long range order in bulk  
69 nanostructures we are convinced that PI-*b*-PFMMA copolymers developed herein are the first

70 examples of functional diblock copolymer consisting of commercially available first block which  
71 makes it readily accessible for scaling up and further investigation.

72

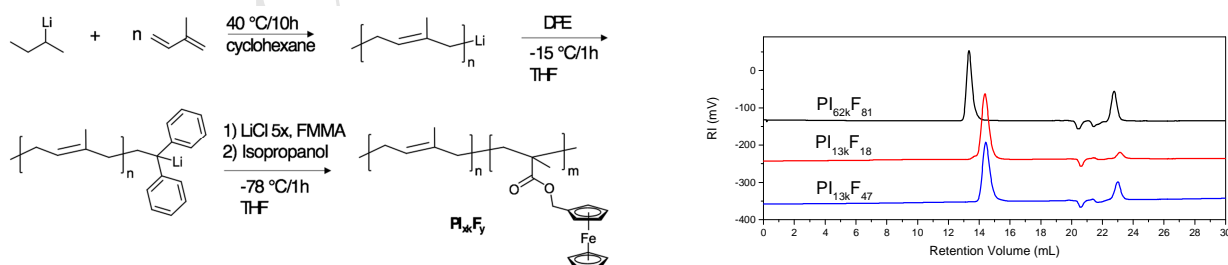
### 73 **Materials and methods**

74 All chemicals were purchased from Sigma-Aldrich unless otherwise stated. Tetrahydrofuran  
75 (THF) was distilled from ketyl radical of benzophenone under argon. Cyclohexane was distilled  
76 from living poly(styryl)lithium under argon. Isoprene was consecutively distilled from calcium  
77 hydride (CaH<sub>2</sub>) and di-*n*-butylmagnesium. FMMA was sublimed 7-10 times using cold finger in the  
78 dark at 0.001 mbar.

79 The PDI was determined by gel permeation chromatography (GPC) using THF with 1%  
80 triethylamine as an eluent at 0.5 ml/min flow rate with a column set consisting of a  
81 precolumn and two 300 x 8 mm main columns (PLgel Mixed C and Mixed D). Rheological  
82 characterization was realized on a Rheometrics solids analyzer (RSA II) operated with a 0.3 mm  
83 gap shear sandwich configuration at 1 % shear strain ( $\gamma$ ) amplitude and 1 rad/s frequency ( $\omega$ ).  
84 Small-angle X-ray scattering (SAXS) profiles were measured using the SAXSLab instrument at the  
85 Niels Bohr Institute (NBI). After synthesis the samples were isolated by precipitation from a good  
86 solvent to a nonsolvent. Such procedure is equivalent to a quenching at infinitely high temperature  
87 and results in disordered bulk morphology. As prepared samples were further used for the SAXS  
88 measurements without additional treatment. The SAXSLab instrument uses a Rigaku 40W micro-  
89 focused Cu-source producing X-rays with a wavelength of 1.54 Å which is detected by a moveable  
90 Pilatus 300k pixel-detector. A sample was mounted in small Cu-discs between two 5-7 μm mica  
91 windows. The sample holder discs were connected to a Linkam HFS91 stage connected to a LNP95  
92 temperature controller enabling temperature scans. Each temperature had a total measurement time  
93 of 15 minutes. The  $q$  calibration of the instrument was done by using silver behenate as a reference.  
94 Two consecutive sets of SAXS measurements were performed on each sample, starting with

95 measurements versus increasing temperatures, followed by a decreasing temperature scan. The  
 96 second set of SAXS measurements was performed to check reproducibility of phases from the first  
 97 set. At each temperature, a total exposure time of 15 minutes was performed in three separate scans  
 98 of 5 minutes.

99 **Anionic polymerization.** The experiments were realized using the anionic polymerization setup  
 100 described elsewhere [17]. In our abbreviation of the block copolymer systems, we will index PI  
 101 with the molar mass of the total diblock copolymer and the PFMMA will be indexed with the  
 102 volume fraction of PFMMA. For the synthesis of PI-*b*-PFMMA diblock copolymer with a total  
 103 molecular weight of 13 kDa, having a volume fraction of PFMMA block of 47%, abbreviated as  
 104 PI<sub>13k</sub>F<sub>47</sub>, the following procedure was adopted. A solution of isoprene (1.2 g) in cyclohexane (0.17  
 105 g/ml) was added to the mixture of *sec*-butyllithium initiator (0.24 mmol, 1x) and 100 ml of  
 106 cyclohexane in 1L reactor and stirred for 10 h at 40 °C (overpressure!). A solution of produced  
 107 living poly(isoprenyl)-Li was transferred to the second reactor containing 0.17 g (0.97, 4x) 1,1-  
 108 diphenyl ethylene (DPE), 0.051 g (1.21 mmol, 5x) LiCl and 200 ml dry THF. After 1 h at -15 °C  
 109 reaction mixture was cooled down to -78 °C and 1.7 g (6.0 mmol) of FMMA was added as a  
 110 solution in THF (0.07 g/ml). Polymerization of the second monomer was conducted for 1 h at -78  
 111 °C, then 2 ml of methanol was added and the diblock copolymer was precipitated to 800 ml  
 112 isopropanol. The precipitant was filtered and dried under vacuum in the dark at 50 °C for 16 h at  
 113 0.001 mbar. Yellowish semisolid product was thereby obtained in a quantitative yield.



114  
 115 Scheme 1. Synthesis of PI-*b*-PFMMA (PI<sub>xk</sub>F<sub>y</sub>) diblock copolymers (left) and the GPC curves (right) corresponding to the obtained  
 116 polymers. In the name of the sample the first subscript denotes total molecular weight of the diblock copolymer while the second  
 117 subscript signifies the average (from NMR and TGA) volume fraction (in %) of the PFMMA block.

118

119

120 **Results and Discussion**

121 **Synthesis.** The synthesis via anionic polymerization of the methacrylate containing monomers  
 122 require intermediate capping of the poly(isoprenyl)lithium with 1,1-diphenyl ethylene to reduce the  
 123 nucleophilicity of the growing centers which would otherwise be active enough towards carbonyl  
 124 groups of the monomer/polymer. Molar excess (5x) of the LiCl compared to initiator was also used  
 125 for the same purpose. In addition, an exhaustive monomer purification was performed either by  
 126 distillation (isoprene) or repetitive sublimation (PFMMA) of the monomers to minimize termination  
 127 of the growing chains with protic impurities. As a consequence, well-defined diblock copolymers  
 128 could be obtained with polydispersities ranging from 1.04 to 1.07 (Table 1).

129 Table 1. Characteristics of the synthesized PFMMA homopolymer and diblock copolymers.

Name <sup>a</sup>	MW, kDa (NMR)	MW PFMMA kDa	PDI (GPC)	Residue at 900°C (TGA), %	$f_{\text{PFMMA}}$ (NMR)	$f_{\text{PFMMA}}$ (TGA)	$f_{\text{PFMMA}}$ average	Unit cell size, nm <sup>b</sup>
PFMMA	45.8	45.8	1.15	25.2	1.00	1.00	1.00	n/a
PI <sub>62k</sub> F <sub>81</sub>	61.5	54.4	1.04	23.6	0.84	0.78	0.81	24.3
PI <sub>13k</sub> F <sub>18</sub>	13.4	3.7	1.06	6.04	0.20	0.15	0.18	16.6
PI <sub>13k</sub> F <sub>47</sub>	12.9	8.4	1.07	13.9	0.55	0.39	0.47	15.9

130

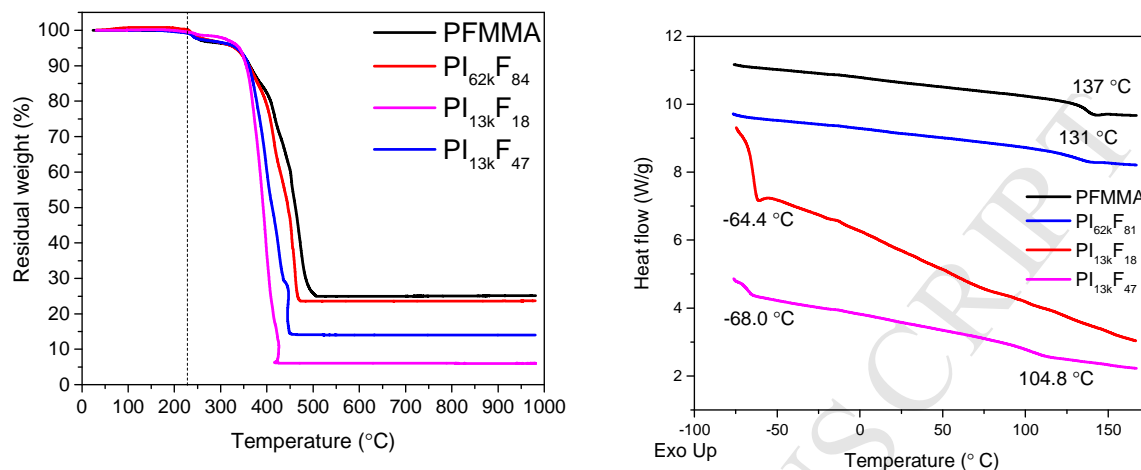
131 <sup>a</sup>In the name of the sample the first subscript denotes total molecular weight of the diblock copolymer while the second subscript  
 132 signifies the average (from NMR and TGA) volume fraction (in %) of the PFMMA block estimated using the density of PFMMA  
 133 and poly(1,4-isoprene) equal to 1.37 g/ml and 0.91 g/ml respectively.

134 <sup>b</sup>Unit cell parameter calculated from SAXS as  $d = 2\pi/q^*$  for lamellar (LAM) and  $a = 2d/\sqrt{3}$  for hexagonally packed cylinders (HEX)  
 135 morphologies where  $q^*$  is the first order reflection.

136

137 **TGA/DSC.** Thermal stability of the PI-PFMMA diblock copolymers was found to be 14-60 °C  
 138 lower compared to PFMMA homopolymer which is attributed to the presence of poly(isoprene) in  
 139 the block copolymer structure. The temperature corresponding to the maximum rate of  
 140 decomposition ( $T_{\text{max}}$ ) is equal to 454 °C for PFMMA while for the diblock copolymers it is within  
 141 the range 390-440 °C (Figure 1). Since upon decomposition PFMMA containing polymers in air  
 142 will form pure Fe<sub>2</sub>O<sub>3</sub> as a residue [2], we could estimate the volume fractions ( $f_{\text{PFMMA}}$ ) of PFMMA  
 143 block from TGA data (see Table 1). The values obtained in such manner were averaged with NMR

144 based volume fractions and thus only the average  $f_{\text{PFMMA}}$  values will be used in the following. All  
 145 three values are given in Table 1.



146

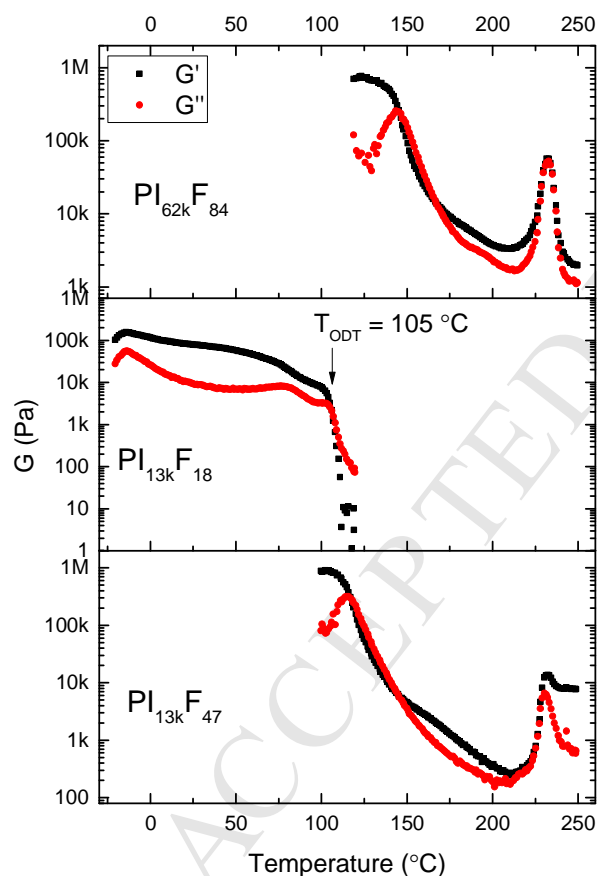
147 Figure 1. TGA (left, in air) and DSC (right, in  $\text{N}_2$ ) curves of the synthesized block copolymers recorded at  $10\text{ }^\circ\text{C}/\text{min}$  demonstrating  
 148 (TGA) plateau after  $\sim 500\text{ }^\circ\text{C}$  due to  $\text{Fe}_2\text{O}_3$  residue and (DSC) glass transition dependence of the diblock copolymer on the  
 149 composition. Only the second DSC scan is shown for every sample. Glass transition temperatures are estimated by curve  
 150 differentiation method.

151

152 DSC data reveal the presence of poly(isoprene) characterized by a low glass transition  
 153 temperature ( $T_g$ ) equal to  $-64.4\text{ }^\circ\text{C}$  and  $-68.0\text{ }^\circ\text{C}$  for the case of  $\text{PI}_{13\text{k}}\text{F}_{18}$  and  $\text{PI}_{13\text{k}}\text{F}_{47}$  respectively.  
 154 Subtle  $T_g$  variations for PI block reflect the influence of the second PFMMA block on the glass  
 155 transition of the first block. Similar phenomena is observed at the high temperature end. Pure  
 156 PFMMA glass transition occurs at  $137\text{ }^\circ\text{C}$  while the presence of PI reduces  $T_g$  to  $131\text{ }^\circ\text{C}$  for  
 157  $\text{PI}_{62\text{k}}\text{F}_{81}$ . Even lower  $T_g$  ( $104.8\text{ }^\circ\text{C}$ ) was found for  $\text{PI}_{13\text{k}}\text{F}_{47}$  which is thought to be caused by low  
 158 molecular weight of the PFMMA block (8.4 kDa). Such phenomena is well-documented for, e.g.,  
 159 poly(styrene) that exhibits  $T_g$  reduction as a function of finitely low chain length [18].

160 **Rheology.** Isochronal temperature scans [19-21] for diblock copolymers are presented in Figure  
 161 2. When the temperature is below  $\sim 140\text{ }^\circ\text{C}$  the polymer chains are in a glassy state which is  
 162 characterized by high storage modulus values ( $10^6\text{ Pa}$ ) and domination of the elastic over viscous  
 163 behavior ( $G' > G''$ ). After the glass transition the chains acquire sufficient mobility and microphase  
 164 separation becomes feasible via diffusion of the PI and PFMMA blocks in the molten state. In the

165 case of PI<sub>62k</sub>F<sub>81</sub> and PI<sub>13k</sub>F<sub>47</sub> the dynamical mechanical spectra look almost identical: gradual  
 166 softening of the polymers occurs until almost liquid-like state is reached at ca. 200 °C followed by a  
 167 crosslinking at higher temperatures. On the other hand, for PI<sub>13k</sub>F<sub>18</sub> sample an interesting  
 168 phenomenon was identified, that is, an order to disorder transition (ODT) occurs at 105 °C  
 169 accompanied by a sharp decrease of both  $G'$  and  $G''$  to negligibly low values which are beyond the  
 170 resolution of our instrument. During ODT the unfavorable interactions between PI and PFMMA  
 171 segments are overcome by an excess of heat supplied to the system at elevated temperature.  
 172 Heterosegmental mixing thus takes place and terminal regime is reached.

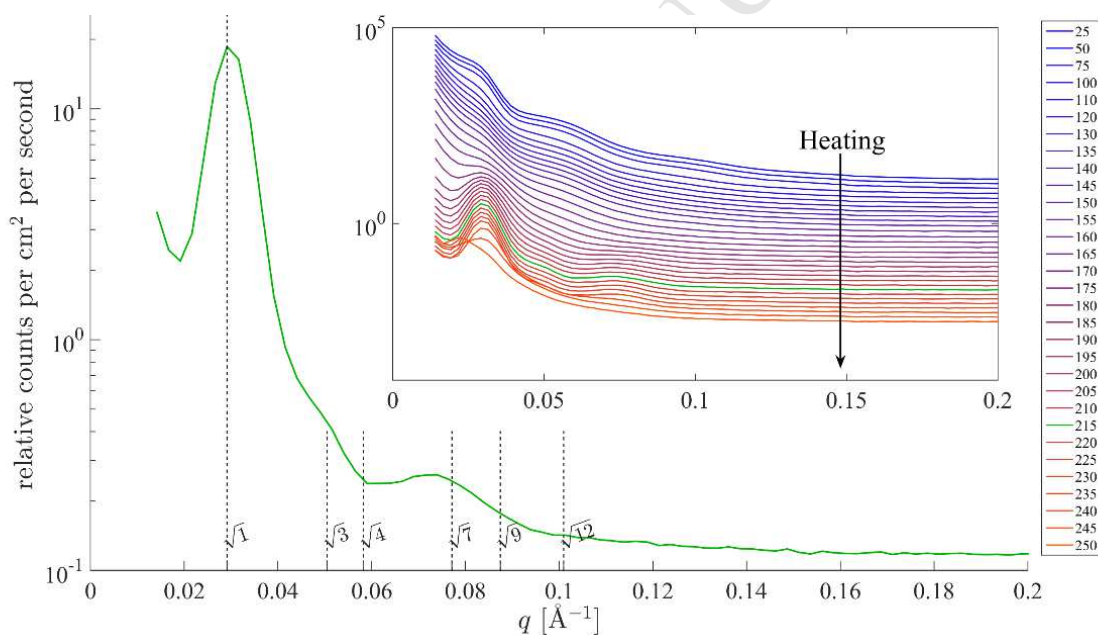


173

174 Figure 2. Isochronal ( $\omega = 1$  rad/s) dynamic storage ( $G'$ ) and loss ( $G''$ ) moduli measured at 2 °C/min heating rate and constant shear  
 175 strain ( $\gamma = 1$  %) showing the glass transition (decrease in  $G'$ ,  $G''$ ), the order-to-disorder transition (sharp drop in  $G'$ ,  $G''$  at 105 °C) as  
 176 well as crosslinking phenomena (increase in  $G'$ ,  $G''$ ).

177 **SAXS.** The scattering profiles at varied temperature for the sample PI<sub>62k</sub>F<sub>81</sub>, are shown on Figure  
 178 3. The data clearly demonstrate the transition from powder scattering below  $T=155$  °C to scattering  
 179 dominated by a broad peak for higher temperatures. At low temperatures, the SAXS data follows a

180  $q^{-3.9}$  power law, which is in a good agreement with the  $q^{-4}$  slope for powdery samples dominated by  
 181 surface scattering. The statistical error-bars on the slope is rather small, below  $\pm 0.002$ , however  
 182 with the relative small  $q$ -range where the Porod-scattering is dominant, the fit result is rather  
 183 dependent on the exact range that is fitted. Including such systematic errors, we estimate the error  
 184 bar to be 0.2. Further increase in the temperature leads to enhanced chain mobility and bulk  
 185 structuring of the sample as exemplified by appearance of higher order reflections. The positions of  
 186 the second and third peaks coincide with hexagonally packed cylinder (HEX) morphology which is  
 187 in agreement with the volume fraction of the PFMMA component (81 %) in the diblock copolymer.  
 188 The missing  $\sqrt{4}$  peak fits well with a form factor minimum from a hexagonal cylinder packing with  
 189 a 24 nm unit cell where the cylinder volume is ca. 20 % as here (minimum around 0.06-0.07  $\text{\AA}^{-1}$ ).



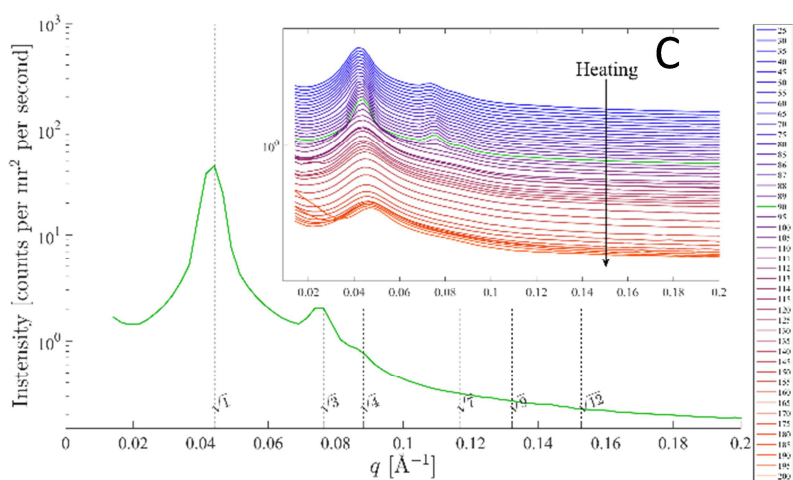
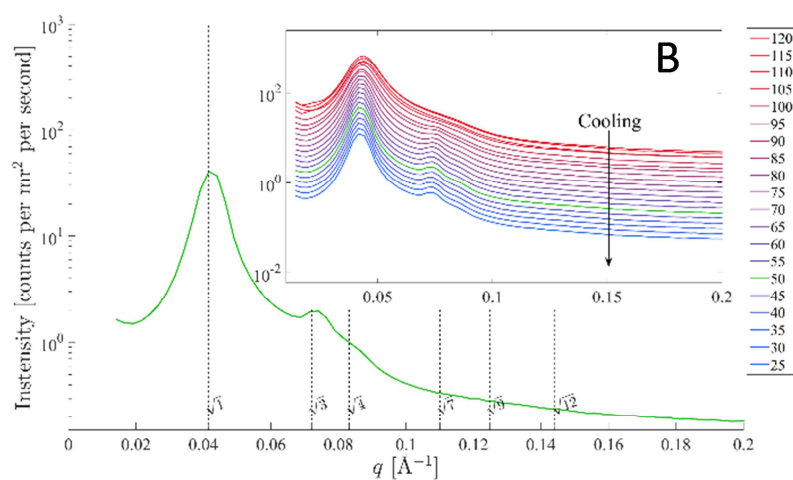
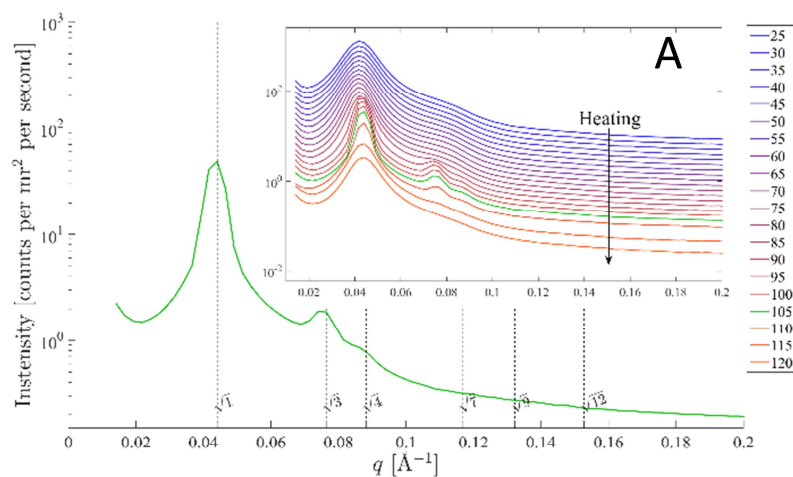
190

191 Figure 3: SAXS data for the sample  $PI_{62k}F_{81}$  acquired at 215 °C with the dashed lines marking relative peak distances for a HEX  
 192 morphology. The inset shows SAXS profiles measured during in-situ temperature scans from 25 to 250 °C.

193

194 SAXS measurements performed at varied temperature for the sample  $PI_{13k}F_{18}$  confirm the  
 195 location of  $T_{ODT}$  between 105 and 110 °C which is in excellent agreement with the rheology data  
 196 (Figure 4). At the proximity to ODT second and third order reflection peaks appear indicating the  
 197 formation of the well-ordered morphology. The relative peak positions ( $q/q^* = 1 : \sqrt{3} : \sqrt{4}$ )  
 198 correspond to the HEX, where PFMMA being the minority domains forms cylinders and majority

199 of PI forms the surrounding matrix. In this case the form factor minimum is shifted out to ca.  $0.1 \text{ \AA}^{-1}$   
 200 <sup>1</sup> so the  $\sqrt{4}$  peak is now visible. The first heating cycle (Figure 4A) was terminated at  $120 \text{ }^\circ\text{C}$  by  
 201 cooling the sample to room temperature to avoid excessive polymer degradation. While cooling,  
 202 disordered, segmentally mixed  $\text{PI}_{13k}\text{F}_{18}$  sample undergoes microphase separation leading to the  
 203 same HEX morphology which becomes permanently fixed after crossing  $T_g$  of the PFMMA block.



204

205 Figure 4. SAXS temperature scans of the PI<sub>13k</sub>F<sub>18</sub> sample acquired at (A) 105 °C, (B) 50 °C and (C) 90 °C. (A) Data from first  
 206 heating cycle showing the transition from disordered to ordered and back to disordered state and (B) first cooling cycle where after  
 207 disorder-to-order transition the microphase separated structure is fixed in a glassy state. Blue lines indicate colder while red indicates  
 208 warmer temperatures. (C) Heating to higher temperature (200 °C) in the second heating cycle to collect more data in the disordered  
 209 state for RPA fitting.

210

211 The second heating cycle (Figure 4C) was terminated at 200 °C and a wide range of data in the  
 212 disordered state above the ODT was acquired. This allowed us to fit the experimental scattering  
 213 data with random phase approximation theory (RPA) and thereby estimate the Flory-Huggins  
 214 interaction parameter,  $\chi$  [22, 23]. The RPA prediction for the scattering intensity of a disordered  
 215 diblock copolymer melt is

$$I(q) = \left( \frac{b_1}{v_1} - \frac{b_2}{v_2} \right)^2 \left[ \frac{S_{11}^0 + S_{22}^0 + 2S_{12}^0}{S_{11}^0 S_{22}^0 - (S_{12}^0)^2} - \frac{2\chi}{v_R} \right]^{-1} \quad (1)$$

216 where  $i = 1, 2$  are indices for the PI and PFMMA blocks respectively,  $v_R$  is a reference volume [24]  
 217 here set to  $v_R = 118 \text{ \AA}^3$  and  $b_i$  and  $v_i$  are the scattering lengths and molecular volumes of the  
 218 polymers calculated as follows:

$$b_i = Z_i r_e \quad (2)$$

$$v_i = \frac{M_{w,i}}{d N_a} \quad (3)$$

220 where  $Z$  is the number of electrons in the monomer  $i$ ,  $r_e$  is the classical Thomson scattering length  
 221 ( $2.82 \times 10^{-13} \text{ cm}$ ),  $M_w$  is the molecular weight of the monomer  $i$ ,  $d$  is the polymer density and  $N_a$  is  
 222 the Avogadro number.

223 Finally,  $S_{ii}^0$  are the correlation functions between the blocks given by

$$S_{ii}^0 = \phi_i N_i v_i P_i(q) \quad (4)$$

224 and

$$S_{12}^0 = (\phi_1 N_1 v_1 \phi_2 N_2 v_2)^{1/2} F_1(q) F_2(q) \quad (5)$$

225 Here  $\phi_i$  and  $N_i$  are the volume fractions and number of monomers of the blocks and  $P_i(q)$   
 226 and  $F_i(q)$  are the intrablock and interblock correlations respectively given by

$$P_i(q) = 2 \frac{\exp(-u_i) - 1 + u_i}{u_i^2} \quad (6)$$

$$F_i(q) = \frac{1 - \exp(-u_i)}{u_i} \quad (7)$$

$$u_i = \frac{q^2 N_i l_i^2}{6} \quad (8)$$

227 where  $l_i$  is the statistical segment length of block  $i$ . All parameters are known (Table 2) except the  
 228 statistical segment length and the  $\chi$ -parameter, thus, these are the parameters to be determined by  
 229 fitting.

230 Table 2. Structural parameters for the PI<sub>13k</sub>F<sub>18</sub> sample used for the  $\chi$  parameter estimation.

Parameter	Value
$v_R$	118 Å <sup>3</sup>
$b_1$	$1.07 \cdot 10^{-3}$ Å
$b_2$	$4.17 \cdot 10^{-3}$ Å
$v_1$	124 Å <sup>3</sup>
$v_2^*$	345 Å <sup>3</sup>
$\phi_1^*$	0.8
$\phi_2^*$	0.2
$N_1$	143
$N_2$	13

231 \*NMR based volume fractions were used.

232 We fit the data to Equation 1 minimizing the square of the residuals using nonlinear  
 233 minimization routines in Matlab. As Equation 1 only applies in the disordered state we only have a  
 234 suitable temperature range for the PI<sub>13k</sub>F<sub>18</sub> sample, where  $T > T_{ODT}$ . We found that the data range  
 235 from 105 °C to 140 °C could be described by a linear fit. Figure 5A shows an example of a fit of the  
 236 first order peak at 130 °C and Figures 5 B, C provide the linear inverse temperature dependence of  
 237 the fitting parameters assuming that the statistical segment lengths of both arms are equal ( $l_1 =$   
 238  $l_2 = l$ ). This analysis gives dependency 9 where  $T$  is in Kelvins:

$$\chi = 0.12 + 0.19/T \quad (9)$$

239

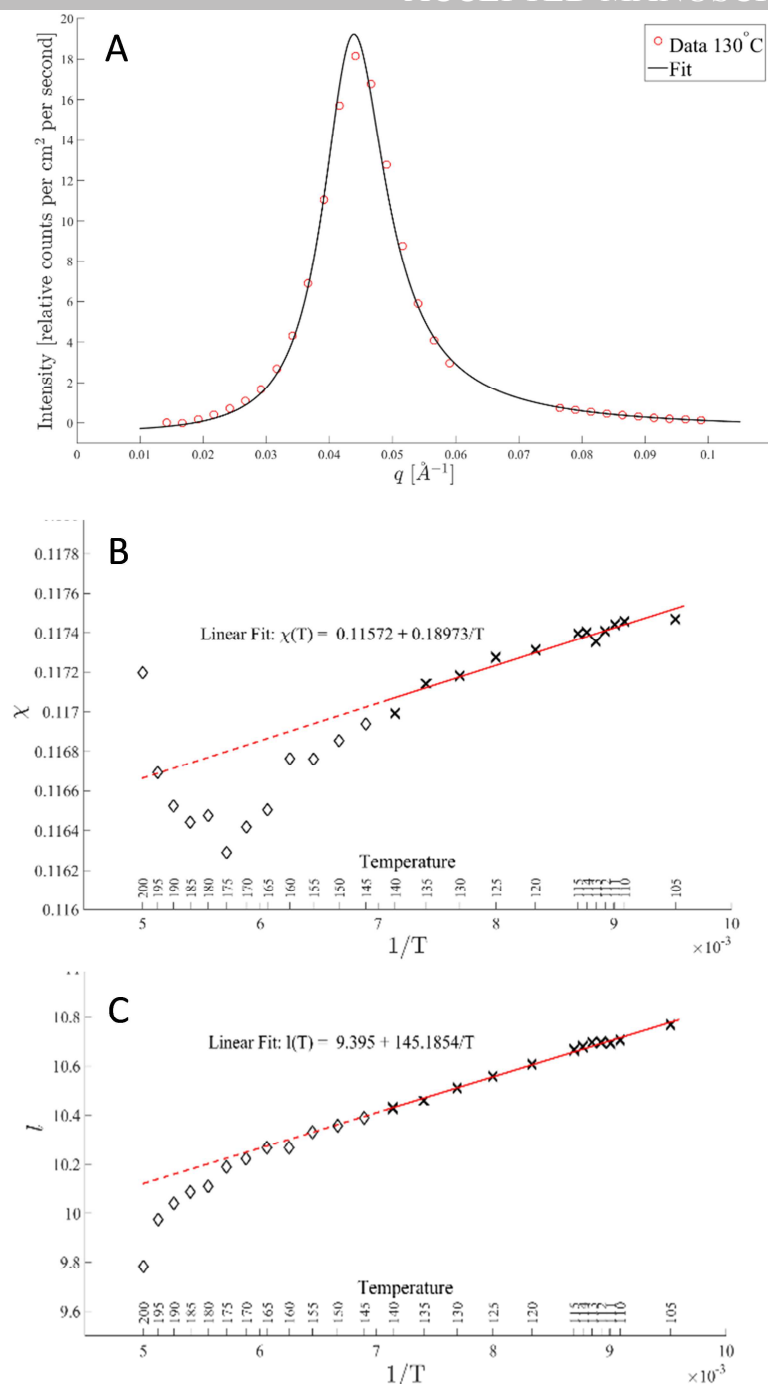


Figure 5. (A) RPA fit of the scattering data from the PI<sub>13k</sub>F<sub>18</sub> sample at 130°C. Temperature dependence of (B)  $\chi$  and (C)  $l$ .

240  
241  
242  
243  
244  
245  
246  
247  
248

The resulting  $\chi$  values and are affected by the background treatment in the SAXS profiles to a minor extent. We found that subtracting the background individually from each SAXS profile using a decaying exponential plus a polynomial of  $n^{\text{th}}$  order plus a constant yielded the most reproducible results. We also found a shoulder on all our measurements at the right-hand side of the primary peak located at around 1.4 times  $q^*$ . Such a shoulder has been observed before [25] and was found on all data sampled in the disordered state with an amplitude inversely proportional to temperature.

249 The origin of this shoulder is composition fluctuations near the ODT as discussed in detail by Bates  
250 et al. [25, 26]. These fluctuations are also shown in Ref. [26] to be persistent for a significant  
251 temperature interval above the order-disorder transition temperature which we confirm here. Such  
252 fluctuations are not accounted for in the mean-field based RPA which will thus not produce the  
253 observed shoulder. Furthermore, the effects from polydispersity in the sample and instrumental  
254 resolution on estimated  $\chi$  values were assessed as described by Almdal et al. [26] and Pedersen et  
255 al. [27] respectively. Accounting for both PDI and instrumental resolution led to negligibly small  
256 variations in the resulting  $\chi$ -values which differed only in the 3<sup>rd</sup> decimal.

257 Hence, from our measurements and analysis at the standard reporting temperature, 150 °C, we  
258 estimate  $\chi_{150^\circ\text{C}} = 0.12$  for the PI-PFMMA pair. Typically 150 °C is chosen as a standard  
259 temperature because it is above  $T_g$  but still below the degradation temperature of most of the known  
260 polymers [24]. The estimated  $\chi$  value ( $\chi_{150^\circ\text{C}} = 0.12$ ) is identical to the PS-P2VP [17] interaction  
261 parameter ( $\chi_{150^\circ\text{C}} = 0.12$ ) but higher than that of PS-PI [28] ( $\chi_{150^\circ\text{C}} = 0.08$ ) and PS-PFS [23]  
262 ( $\chi_{150^\circ\text{C}} = 0.03$ ) pairs indicating significant incompatibility between PI and PFMMA segments.

263 Moreover, our analysis suggests that the average statistical segment length,  $l$ , is in the range 10.0  
264 - 10.7 Å, which agrees well with the values previously reported by Eitouni et al. [23] who also  
265 investigated diblock copolymers of poly(styrene-*b*-ferrocenyldimethylsilane) from the  
266 organometallic group.

267 SAXS measurements performed at different temperatures for the sample PI<sub>13k</sub>F<sub>47</sub> shows relative  
268 featureless scattering (Figure 6). Only in a narrow temperature range between 205 °C – 210 °C,  
269 some higher-order peaks are observed around  $q = 0.075$  and  $0.13 \text{ \AA}^{-1}$ . The structure associated with  
270 these peaks suggests a lamellar morphology as would be expected for a diblock copolymer with  
271 symmetric composition.

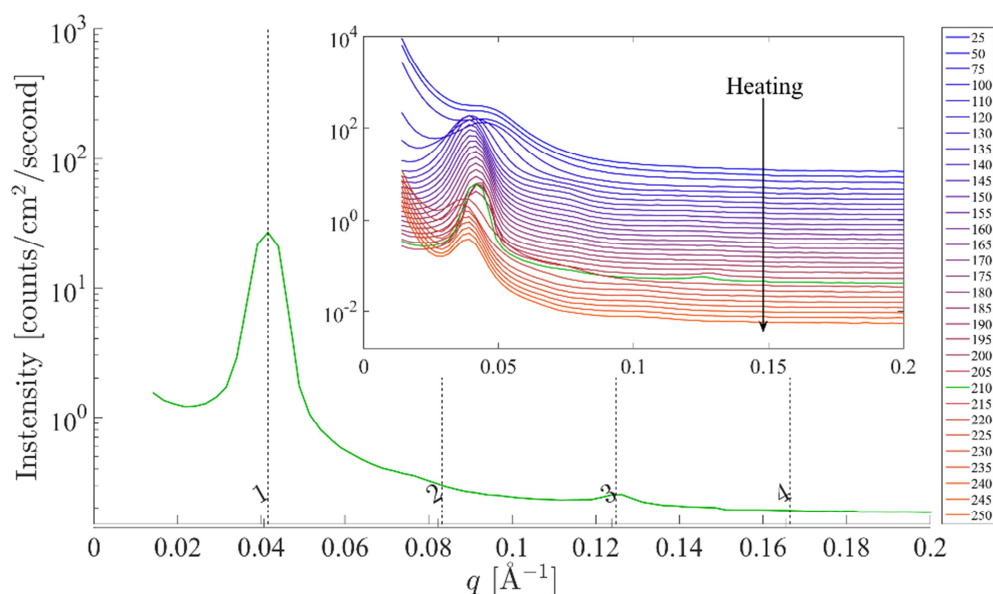
272

273

274

275

276



277 Figure 6: X-ray scattering profile acquired at 210 °C for the PI<sub>13k</sub>F<sub>47</sub> sample demonstrating higher-order reflections at  $q = 0.075 \text{ \AA}^{-1}$   
 278 and  $q = 0.13 \text{ \AA}^{-1}$  which match the relative peak positions (represented by vertical dashed lines) of lamellae morphology. The inset  
 279 shows SAXS profiles measured during in-situ temperature scans from 25 to 250 °C.

280

## 281 Conclusions

282 Synthesized PI-*b*-PFMMA copolymers were subjected to temperature scans while monitoring  
 283 SAXS intensity in-situ. The PI-*b*-PFMMA sample characterized by a lowest MW of PFMMA block  
 284 equal to 3700 g/mol exhibited the presence of an order-to-disorder transition at 105 °C. This  
 285 allowed us to derive a generally accepted dependency of the Flory-Huggins interaction parameter  
 286 ( $\chi$ ) on temperature. Apart from fundamental interest about thermodynamic incompatibility between  
 287 PI and PFMMA components, knowing absolute value of  $\chi$  at a given temperature allows anyone to  
 288 predict an equilibrium domain spacing, pitch size and minimum molecular weight which would be  
 289 required to achieve microphase separation in bulk [24].

290

## 291 Acknowledgements

292 Authors are thankful to Villum Foundation for the financial support of the project.

293

294

295 **References**

- 296 [1] C.U. Pittman, J.C. Lai, D.P. Vanderpool, Kinetics of Ferrocenylmethyl Acrylate and  
297 Ferrocenylmethyl Methacrylate Polymerization. Preparation of Polymeric Ferricinium Salts,  
298 *Macromolecules* 3(1) (1970) 105-107.
- 299 [2] S. Chernyy, Z. Wang, J.J.K. Kirkensgaard, A. Bakke, K. Mortensen, S. Ndoni, K. Almdal,  
300 Synthesis and Characterization of Ferrocene Containing Block Copolymers, *J. Polym. Sci., Part A:*  
301 *Polym. Chem.* In press (2016) DOI: 10.1002/pola.28435.
- 302 [3] R.L.N. Hailles, A.M. Oliver, J. Gwyther, G.R. Whittell, I. Manners, Polyferrocenylsilanes:  
303 synthesis, properties, and applications, *Chem. Soc. Rev.* 45(19) (2016) 5358-5407.
- 304 [4] R. Sun, L. Wang, H. Yu, Z.-u. Abdin, Y. Chen, J. Huang, R. Tong, Molecular Recognition and  
305 Sensing Based on Ferrocene Derivatives and Ferrocene-Based Polymers, *Organometallics* 33(18)  
306 (2014) 4560-4573.
- 307 [5] M. Saleem, H. Yu, L. Wang, A. Zain ul, H. Khalid, M. Akram, N.M. Abbasi, J. Huang, Review  
308 on synthesis of ferrocene-based redox polymers and derivatives and their application in glucose  
309 sensing, *Anal. Chim. Acta* 876(Supplement C) (2015) 9-25.
- 310 [6] E.S. Beh, D. De Porcellinis, R.L. Gracia, K.T. Xia, R.G. Gordon, M.J. Aziz, A Neutral pH  
311 Aqueous Organic–Organometallic Redox Flow Battery with Extremely High Capacity Retention,  
312 *ACS Energy Letters* 2(3) (2017) 639-644.
- 313 [7] S. Kaur, S. Dhoun, G. Depotter, P. Kaur, K. Clays, K. Singh, Synthesis, linear and nonlinear  
314 optical properties of thermally stable ferrocene-diketopyrrolopyrrole dyads, *RSC Advances* 5(103)  
315 (2015) 84643-84656.
- 316 [8] J. Shi, C.J.W. Jim, F. Mahtab, J. Liu, J.W.Y. Lam, H.H.Y. Sung, I.D. Williams, Y. Dong, B.Z.  
317 Tang, Ferrocene-Functionalized Hyperbranched Polyphenylenes: Synthesis, Redox Activity, Light  
318 Refraction, Transition-Metal Complexation, and Precursors to Magnetic Ceramics, *Macromolecules*  
319 43(2) (2010) 680-690.
- 320 [9] M. Hmyene, A. Yassar, M. Escorne, A. Percheron-Guegan, F. Garnier, Magnetic properties of  
321 ferrocene-based conjugated polymers, *Adv. Mater.* 6(7-8) (1994) 564-568.
- 322 [10] R.G.H. Lammertink, M.A. Hempenius, V.Z.H. Chan, E.L. Thomas, G.J. Vancso,  
323 Poly(ferrocenyldimethylsilanes) for Reactive Ion Etch Barrier Applications, *Chem. Mater.* 13(2)  
324 (2001) 429-434.
- 325 [11] J.C. Lai, T.D. Rounsefell, C.U. Pittman, Copolymerization of Ferrocenylmethyl Acrylate and  
326 Ferrocenylmethyl Methacrylate with Organic Monomers, *Macromolecules* 4(2) (1971) 155-161.
- 327 [12] C.U. Pittman, A. Hirao, Anionic homopolymerization of ferrocenylmethyl methacrylate, *J.*  
328 *Polym. Sci. A Polym. Chem.* 15(7) (1977) 1677-1686.
- 329 [13] M. Gallei, B.V. Schmidt, R. Klein, M. Rehahn, Defined Poly[styrene-block-(ferrocenylmethyl  
330 methacrylate)] Diblock Copolymers via Living Anionic Polymerization, *Macromol. Rapid*  
331 *Commun.* 30(17) (2009) 1463-1469.
- 332 [14] C.M. Bates, M.J. Maher, D.W. Janes, C.J. Ellison, C.G. Willson, Block Copolymer  
333 Lithography, *Macromolecules* 47(1) (2014) 2-12.
- 334 [15] M.D. Rodwogin, C.S. Spanjers, C. Leighton, M.A. Hillmyer,  
335 Polylactide–Poly(dimethylsiloxane)–Polylactide Triblock Copolymers as Multifunctional Materials  
336 for Nanolithographic Applications, *ACS Nano* 4(2) (2010) 725-732.
- 337 [16] M.W. Matsen, F.S. Bates, Unifying Weak- and Strong-Segregation Block Copolymer  
338 Theories, *Macromolecules* 29(4) (1996) 1091-1098.

- 339 [17] M.F. Schulz, A.K. Khandpur, F.S. Bates, K. Almdal, K. Mortensen, D.A. Hajduk, S.M.  
340 Gruner, Phase Behavior of Polystyrene–Poly(2-vinylpyridine) Diblock Copolymers,  
341 *Macromolecules* 29(8) (1996) 2857-2867.
- 342 [18] P. Claudy, J.M. L  toff  , Y. Camberlain, J.P. Pascault, Glass transition of polystyrene versus  
343 molecular weight, *Polym. Bull.* 9(4) (1983) 208-215.
- 344 [19] J. Zhao, B. Majumdar, M.F. Schulz, F.S. Bates, K. Almdal, K. Mortensen, D.A. Hajduk, S.M.  
345 Gruner, Phase Behavior of Pure Diblocks and Binary Diblock Blends of  
346 Poly(ethylene)–Poly(ethylethylene), *Macromolecules* 29(4) (1996) 1204-1215.
- 347 [20] S. Foerster, A.K. Khandpur, J. Zhao, F.S. Bates, I.W. Hamley, A.J. Ryan, W. Bras, Complex  
348 phase behavior of polyisoprene-polystyrene diblock copolymers near the order-disorder transition,  
349 *Macromolecules* 27(23) (1994) 6922-6935.
- 350 [21] J.L. Adams, W.W. Graessley, R.A. Register, Rheology and the microphase separation  
351 transition in styrene-isoprene block copolymers, *Macromolecules* 27(21) (1994) 6026-6032.
- 352 [22] C.C. Lin, S.V. Jonnalagadda, P.K. Kesani, H.J. Dai, N.P. Balsara, Effect of Molecular  
353 Structure on the Thermodynamics of Block Copolymer Melts, *Macromolecules* 27(26) (1994)  
354 7769-7780.
- 355 [23] H.B. Eitouni, N.P. Balsara, H. Hahn, J.A. Pople, M.A. Hempenius, Thermodynamic  
356 Interactions in Organometallic Block Copolymers: Poly(styrene-block-ferrocenyldimethylsilane),  
357 *Macromolecules* 35(20) (2002) 7765-7772.
- 358 [24] C. Sinturel, F.S. Bates, M.A. Hillmyer, High  $\chi$ –Low N Block Polymers: How Far Can We  
359 Go?, *ACS Macro Letters* 4(9) (2015) 1044-1050.
- 360 [25] F.S. Bates, J.H. Rosedale, G.H. Fredrickson, Fluctuation effects in a symmetric diblock  
361 copolymer near the order–disorder transition, *J. Chem. Phys.* 92(10) (1990) 6255-6270.
- 362 [26] K. Almdal, F.S. Bates, K. Mortensen, Order, disorder, and fluctuation effects in an asymmetric  
363 poly(ethylene-propylene)-poly(ethylethylene) diblock copolymer, *J. Chem. Phys.* 96(12) (1992)  
364 9122-9132.
- 365 [27] J.S. Pedersen, D. Posselt, K. Mortensen, Analytical treatment of the resolution function for  
366 small-angle scattering, *J. Appl. Crystallogr.* 23(4) (1990) 321-333.
- 367 [28] A.K. Khandpur, S. Foerster, F.S. Bates, I.W. Hamley, A.J. Ryan, W. Bras, K. Almdal, K.  
368 Mortensen, Polyisoprene-Polystyrene Diblock Copolymer Phase Diagram near the Order-Disorder  
369 Transition, *Macromolecules* 28(26) (1995) 8796-8806.

370

371

- Poly(isoprene-*b*-ferrocenylmethyl methacrylate) diblock copolymers are investigated
- Order-to-disorder transition is detected for 13400 g/mol sample at 105 °C
- Random phase approximation theory could therefore be applied
- Dependency of the Flory-Huggins interaction parameter on temperature is derived

ACCEPTED MANUSCRIPT